

Significant increase in thermal conductivity of cathode material $LiFePO_4$ by Na substitution： A machine learning interatomic potential-assisted investigation

Shi-Yi Li(李诗怡), Qian Liu(刘骞), Yu-Jia Zeng(曾育佳), Guofeng Xie(谢国锋), and Wu-Xing Zhou(周五星)
Citation: Chin. Phys. B, 2025, 34 (**2**): 028201. DOI: 10.1088/1674-1056/ad9e99
Journal homepage: http://cpb.iphy.ac.cn; http://iopscience.iop.org/cpb

What follows is a list of articles you may be interested in

Defect chemistry engineering of Ga-doped garnet electrolyte with high stability for solid-state lithium metal batteries

Sihan Chen(陈思汗), Jun Li(黎俊), Keke Liu(刘可可), Xiaochen Sun(孙笑晨), Jingwei Wan(万京伟), Huiyu Zhai(翟慧宇), Xinfeng Tang(唐新峰), and Gangjian Tan(谭刚健)
Chin. Phys. B, 2024, 33 (**8**): 088203. DOI: 10.1088/1674-1056/ad41b9

Surface encapsulation of layered oxide cathode material with $NiTiO_3$ for enhanced cycling stability of Na-ion batteries

Zilin Hu(胡紫霖), Bin Tang(唐彬), Ting Lin(林挺), Chu Zhang(张楚), Yaoshen Niu(牛耀申), Yuan Liu(刘渊), Like Gao(高立克), Fei Xie(谢飞), Xiaohui Rong(容晓晖), Yaxiang Lu(陆雅翔), and Yongsheng Hu(胡勇胜)
Chin. Phys. B, 2024, 33 (**8**): 088202. DOI: 10.1088/1674-1056/ad50c2

Stress effect on lattice thermal conductivity of anode material $NiNb_2O_6$ for lithium-ion batteries

Ao Chen(陈奥), Hua Tong(童话), Cheng-Wei Wu(吴成伟), Guofeng Xie(谢国锋), Zhong-Xiang Xie(谢忠祥), Chang-Qing Xiang(向长青), and Wu-Xing Zhou(周五星)
Chin. Phys. B, 2023, 32 (**5**): 058201. DOI: 10.1088/1674-1056/acaa2d

Tuning hybrid liquid/solid electrolytes by lowering Li salt concentration for lithium batteries

Wei Yang(杨伟), Qi-Di Wang(王启迪), Yu Lei(雷宇), Zi-Pei Wan(万子裴), Lei Qin(秦磊), Wei Yu(余唯), Ru-Liang Liu(刘如亮), Deng-Yun Zhai(翟登云), Hong Li(李泓), Bao-Hua Li(李宝华), Fei-Yu Kang(康飞宇)
Chin. Phys. B, 2018, 27 (**6**): 068201. DOI: 10.1088/1674-1056/27/6/068201

Concentrated dual-salt electrolytes for improving the cycling stability of lithium metal anodes

Pin Liu(刘品), Qiang Ma(马强), Zheng Fang(方铮), Jie Ma(马洁), Yong-Sheng Hu(胡勇胜), Zhi-Bin Zhou(周志彬), Hong Li(李泓), Xue-Jie Huang(黄学杰), Li-Quan Chen(陈立泉)
Chin. Phys. B, 2016, 25 (**7**): 078203. DOI: 10.1088/1674-1056/25/7/078203

Significant increase in thermal conductivity of cathode material $LiFePO_4$ by Na substitution: A machine learning interatomic potential-assisted investigation

Shi-Yi Li(李诗怡), Qian Liu(刘骞), Yu-Jia Zeng(曾育佳), Guofeng Xie(谢国锋)[†], and Wu-Xing Zhou(周五星)[‡]

School of Materials Science and Engineering, Hunan Provincial Key Laboratory of Advanced Materials for New Energy Storage and Conversion, Hunan University of Science and Technology, Xiangtan 411201, *China*

(Received 26 September 2024; revised manuscript received 29 November 2024; accepted manuscript online 13 December 2024)

$LiFePO_4$ is a cathode material with good thermal stability, but low thermal conductivity is a critical problem. In this study, we employ a machine learning potential approach based on first-principles methods combined with the Boltzmann transport theory to investigate the influence of Na substitution on the thermal conductivity of $LiFePO_4$ and the impact of Li-ion de-embedding on the thermal conductivity of $Li_{3/4}Na_{1/4}FePO_4$, with the aim of enhancing heat dissipation in Li-ion batteries. The results show a significant increase in thermal conductivity due to an increase in phonon group velocity and a decrease in phonon anharmonic scattering by Na substitution. In addition, the thermal conductivity increases significantly with decreasing Li-ion concentration due to the increase in phonon lifetime. Our work guides the improvement of the thermal conductivity of $LiFePO_4$, emphasizing the crucial roles of both substitution and Li-ion detachment/intercalation for the thermal management of electrochemical energy storage devices.

Keywords: lattice thermal conductivity, machine learning potential, $LiFePO_4$

PACS: 82.47.Aa, 74.25.fc, 44.10.+I, 66.70.–f

DOI: 10.1088/1674-1056/ad9e99 **CSTR:** 32038.14.CPB.ad9e99

1. Introduction

Li-ion batteries are widely used in portable electronic products due to their small size, light weight and high energy density.[1–4] The cathode materials of Li-ion batteries are developing towards the direction of high energy density, long cycle life, low cost and being environmentally friendly.[5] $LiFePO_4$ is of great interest due to its low cost, long service life and high thermal stability.[6,7] Unfortunately, $LiFePO_4$ also has significant disadvantages; for example, at room temperature the electronic conductivity (10^{-9}–10^{-10} $cm^2{\cdot}S^{-1}$) and Li-ion diffusion rate (10^{-14}–10^{-16} $cm^2{\cdot}S^{-1}$) are low, leading to the poor electrochemical performance.[8] To address these issues, doping with isovalent cations was found to be a very effective method, thus Na substitution at the Li sites of $LiFePO_4$ is expected to improve its electrochemical performance.[9] $LiFePO_4$ absorbs and releases energy by disengaging and intercalating Li^+ and electrons. When Na^+ is doped, the *b* lattice constant decreased from 6.04 Å to 5.86 Å, enhancing Li^+ intercalation/de-intercalation and accelerating Li-ion diffusion.[10] After Na^+ doping, Na^+ has lower activity than Li^+ and remains in position, supporting one-dimensional channels that strengthen the crystal structure of the material and improve the cycling performance.[11] The impedance of the Na-doped electrode is significantly reduced and the slope increases in the low-frequency region, indicating that Na doping effectively improves the electrode conductivity and Li-ion mobility. The charge–discharge data show that a small amount of Na^+ doping improves the electrochemical performance, exhibiting good rate capacity and cycle stability, namely, good lattice parameters and conductivity enhancement.[12,13]

In addition, the internal heat generation during the battery charge–discharge process increases significantly.[14] If the heat is not dissipated in a timely manner it can cause battery overheating and even safety issues. Therefore, developing a strategy for improving the heat dissipation of Li-ion batteries is crucial for their safety and future development.[15–21] Feng *et al.* employed quantum computational methods, including high-order lattice anharmonicity, and found that the thermal conductivity κ of Li_xTMO_2 materials was significantly lower than previously believed. De-lithiation further reduced the thermal conductivity of $LiCoO_2$ and $LiNbO_2$ by 40%–70%.[15] Qian *et al.* used molecular dynamics simulations to calculate the thermal conductivity of Li–graphite intercalation compounds (Li_xC_6). They discovered that Li intercalation has an anisotropic effect on thermal conductivity and provided the first atomic-scale insights into the impact of Li intercalation on the phonon spectral properties of graphite.[17] However, the huge computational cost of first-principles theoretical studies and the accuracy of classical molecular dynamics studies are limited by empirical potentials, so the effect

[†]Corresponding author. E-mail: gfxie@xtu.edu.cn

[‡]Corresponding author. E-mail: wuxingzhou@hnu.edu.cn

© 2025 Chinese Physical Society and IOP Publishing Ltd. All rights, including for text and data mining, AI training, and similar technologies, are reserved.

of Na substitution on the thermal conductivity of $LiFePO_4$ remains to be explored. Therefore, in this work we use the machine learning potential based on the first-principles combined with the phonon Boltzmann transport equation (PBTE) to systematically study the thermal conductivity of $LiFePO_4$ and the effects of Na substitution for Li on thermal conductivity. The results showed that Na substitution at one Li site of $LiFePO_4$ significantly enhances the phonon thermal conductivity, from 0.37 $W{\cdot}m^{-1}{\cdot}K^{-1}$ to 7.8 $W{\cdot}m^{-1}{\cdot}K^{-1}$, a 21-fold increase.

2. Model and methodology

The conventional unit cell of $LiFePO_4$ has an orthogonal olivine structure (space group *Pnma*)[22,23] with 28 atoms, comprising four Li, four Fe, four P and 16 O atoms, where the four Li atoms are equivalent, as shown in Fig. 1. In the crystal structure, a P atom occupies the center of a tetrahedron, the Fe^{2+} ions coordinate with the neighboring O atoms to form octahedral units (FeO_6), the octahedral units are corner sharing, and the tetrahedral units (PO_4^{3-}) are edge and corner sharing with the FeO_6 units.[24]

In this work, we substituted Na for Li, and investigated the influence of Na substitution on the thermal conductivity of $LiFePO_4$. The first-principles calculations based on density functional theory (DFT) were implemented on the Vienna *ab initio* simulation package (VASP).[25–27] We selected the generalized gradient approximation (GGA) with the Perdew–Burke–Ernzerhof exchange correlation function,[28] and the plane wave cutoff energy was set to 550 eV. For the geometric optimization, all crystal structures were fully relaxed with a $6\times5\times4$ *k*-point grid, and the convergence criteria for the energy and forces were set to 10^{-6} eV and 10^{-4} $eV{\cdot}Å^{-1}$, respectively. To implement the moment tensor potentials (MTP), a 400-step *ab initio* molecular dynamics simulation with a time step of 1 fs and a temperature of 50–800 K was used as a training set for the machine-learning interatomic potential package.[29–31] During the MTP training process, the weights of energy, force and stress were 1, 0.1 and 0.001, respectively. We examined the root mean square error of energy and force between the MTP and DFT calculations, as shown in Fig. S1 of the supporting material, which indicated that our machine learning-trained potential function was sufficiently precise to reproduce the interatomic interactions of the DFT. Furthermore, we performed molecular dynamics simulations over 400 ps. The energy of $LiFePO_4$ and $Li_{3/4}Na_{1/4}FePO_4$ versus simulation time is illustrated in Fig. S2 of the supporting material, which show that the trained machine learning potential indeed provided a dynamically stable system. The MTP can be used to avoid the huge computational cost associated with the DFT to calculate the second-order force constants (2^{nd}FCs) and the third-order force constants (3^{rd}FCs). In addition, the 2^{nd}FCs, phonon dispersion and phonon density of states were obtained using the MTPs combined with the Phonopy software package[32] with a $3\times3\times2$ supercell based on the finite displacement method, while the 3^{rd}FCs were calculated using the MTPs with a $3\times3\times2$ supercell and the third nearest-neighboring atom as the cutoff radius. Moreover, based on 2^{nd}FCs, and 3^{rd}FCs, the lattice thermal conductivity can be obtained by solving the phonon Boltzmann transport equation via the ShengBTE package[33–37] with $9\times9\times9$ *k*-point grid to ensure the convergence. In addition, in order to discuss the accuracy of MTP, we compare the phonon dispersion relations of $LiFePO_4$ and $Li_{3/4}Na_{1/4}FePO_4$ calculated by DFT and MTP, and find that they are consistent with each other, as shown in Fig. S3 of the supporting material. This means that MTP can accurately describe the $LiFePO_4$ and $Li_{3/4}Na_{1/4}FePO_4$ systems.

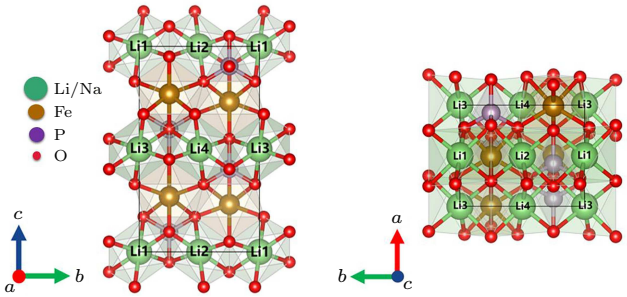


Fig. 1. The structures of $LiFePO_4$: the green spheres represent the Li atoms, the brown spheres represent the Fe atoms, the purple spheres represent the P atoms and the red spheres represent the O atoms.

3. Results and discussion

As shown in Fig. 1, $LiFePO_4$ has four sites for the Li atom, which are marked as Li1, Li2, Li3 and Li4. We substituted one and two Na atoms for Li atoms at these four different sites respectively and calculated the thermal conductivity of $Li_{3/4}Na_{1/4}FePO_4$ and $Li_{1/2}Na_{1/2}FePO_4$ along the *a*, *b* and *c* directions from 100 K to 800 K, as shown in Fig. S4 of the supporting material. The trends of the thermal conductivities along the *a*, *b* and *c* directions are the same, and the thermal conductivities along the *b* direction are chosen for the subsequent analysis. From Fig. 2(a) it is clear that Na substitution significantly enhances the phonon thermal conductivity of $LiFePO_4$. At 300 K (room temperature), $LiFePO_4$ has a very low thermal conductivity of 0.37 $W{\cdot}m^{-1}{\cdot}K^{-1}$, while $Li_{3/4}Na_{1/4}FePO_4$ has a high thermal conductivity of 7.8 $W{\cdot}m^{-1}{\cdot}K^{-1}$, a 21-fold increase. Moreover, we know that the site where Na substitutes for Li has no influence on thermal conductivity of $Li_{3/4}Na_{1/4}FePO_4$, and the thermal conductivity of $Li_{3/4}Na_{1/4}FePO_4$ is higher than that of $Li_{1/2}Na_{1/2}FePO_4$. In our calculated temperature range, it is shown that the lattice thermal conductivity of all samples decreases with increasing temperature due to the intrinsic Umklapp phonon scattering.[38]

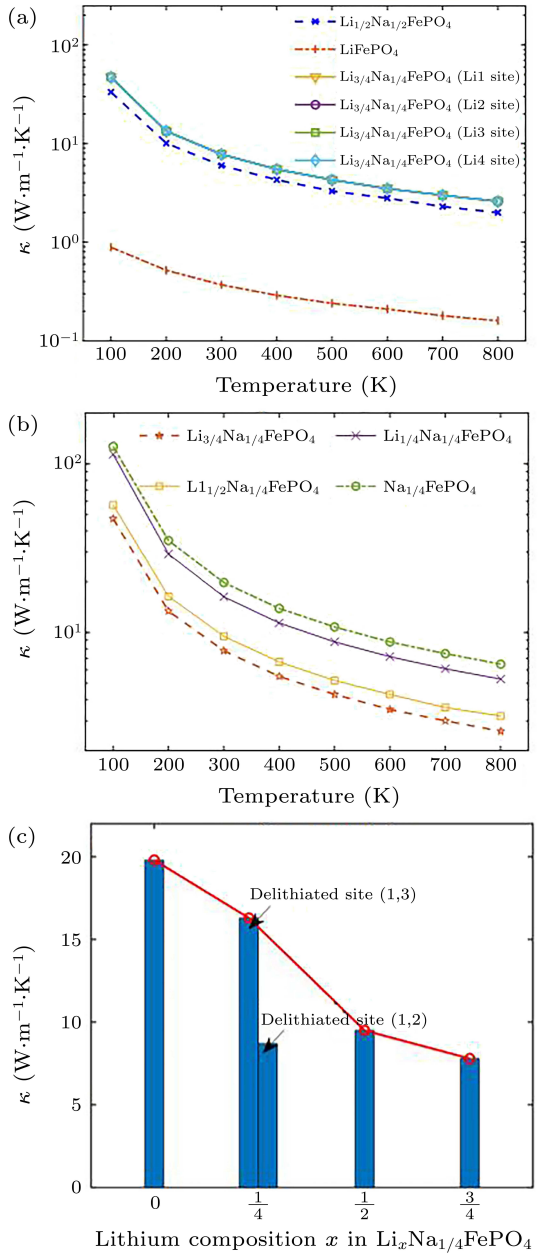


Fig. 2. (a) Lattice thermal conductivity of $Li_xNa_{(1-x)}FePO_4$ ($x = 1$, 3/4, 1/2) along the b direction as a function of temperature. (b) Lattice thermal conductivity of $Li_xNa_{1/4}FePO_4$ ($x = 3/4$, 1/2, 1/4, 0) along the b direction as a function of temperature. (c) Lattice thermal conductivity of $Li_xNa_{1/4}FePO_4$ ($x = 3/4$, 1/2, 1/4, 0) along the b direction at 300 K.

To further study the thermal conductivity of $Li_{3/4}Na_{1/4}FePO_4$ and the delithiation-induced heat transfer mechanism, we calculated the lattice thermal conductivity of $Li_xNa_{1/4}FePO_4$ ($x = 3/4$, 1/2, 1/4, 0) along the b direction from 100 K to 800 K, as shown in Fig. 2(b). Moreover, we removed a certain number of Li atoms to simulate the detachment process and plotted the lattice thermal conductivity of $Li_xNa_{1/4}FePO_4$ versus Li concentration x at 300 K, as shown in Fig. 2(c). According to the structural properties of $Li_{3/4}Na_{1/4}FePO_4$, the chemical environment of the three Li atoms is equal. The thermal conductivity is the same no matter which Li ion is removed. When two Li ions are removed, there are two different configurations depending on the location of the removed Li ions. In Fig. 2(c), the thermal conductivity monotonically decreases as the Li-ion concentration increases, and there is an anomalous phenomenon when two Li ions are removed: when removing Li ions from sites 1 and 2, the thermal conductivity significantly decreases compared with the other structure at the same Li concentration.

In order to understand the origin of the remarkable increase in thermal conductivity of Na substitution $LiFePO_4$, we calculated the phonon dispersion of $LiFePO_4$ and $Li_{3/4}Na_{1/4}FePO_4$ based on MTP, as shown in Fig. 3. There is no imaginary frequency in the phonon dispersions in Figs. 3(a) and 3(b), illustrating that the structures are dynamically stable. In the low-frequency region, the phonon vibration frequency of $Li_{3/4}Na_{1/4}FePO_4$ is higher than that of $LiFePO_4$, which means that acoustic phonons of $Li_{3/4}Na_{1/4}FePO_4$ have a higher group velocity than those of $LiFePO_4$. The group velocity of each phonon mode is calculated by $v_{\lambda,\boldsymbol{q}} = \partial\omega_{\lambda,\boldsymbol{q}}/\partial\boldsymbol{q}$, and the group velocities of acoustic phonons (LA), transverse acoustic phonons (TA1 and TA2) and optical phonons (OPITCAL) along the b direction are plotted in Figs. 3(c) and 3(d). It is obvious that the acoustic phonon velocity of $Li_{3/4}Na_{1/4}FePO_4$ is significantly higher than that of $LiFePO_4$, especially LA phonons. Based on PBTE, lattice thermal conductivity in the i direction can be expressed as $\kappa_{l,i} = \sum_{\lambda,\boldsymbol{q}} C_{\text{ph}} v^2_{\text{g},i}(\lambda,\boldsymbol{q})\tau(\lambda,\boldsymbol{q})$; the summation is over all phonon modes with wave vector $\boldsymbol{q}$ and dispersion branch λ, C_{ph} is the mode volumetric specific heat, $v_{\text{g,i}}(\lambda,\boldsymbol{q})$ is the ith component of the group velocity vector and $\tau(\lambda,\boldsymbol{q})$ is the lifetime of the phonon mode with wave vector $\boldsymbol{q}$ and dispersion branch λ.[39–42] The thermal conductivity of each phonon mode is proportional to the square of the phonon group velocity, therefore the larger group velocity of acoustic phonons in $Li_{3/4}Na_{1/4}FePO_4$ is one of the key reasons for the much higher thermal conductivity of $Li_{3/4}Na_{1/4}FePO_4$.

From the above expression, it is known that the thermal conductivity of each phonon mode is proportional to the phonon lifetime $\tau(\lambda,\boldsymbol{q})$. The Grüneisen parameter and lifetime of each phonon mode in $LiFePO_4$ and $Li_{3/4}Na_{1/4}FePO_4$ are shown in Figs. 3(e) and 3(f), respectively. Generally, a large Grüneisen parameter indicates strong phonon–phonon anharmonic scattering and is responsible for a low lifetime and low thermal conductivity.[43] It is clear in Figs. 3(e) and 3(f) that the Grüneisen parameter of $Li_{3/4}Na_{1/4}FePO_4$ is lower, which results in a higher phonon lifetime and a significant improvement in thermal conductivity.

Moreover, deintercalation/intercalation of Li ions occurs repeatedly in the cathode during the charging and discharging process and the thermal conductivity of cathode material will vary with changes in Li-ion concentration. To shed light on the origin of the change in the thermal conductivity

of $Li_{3x/4}Na_{1/4}FePO_4$ with the degree of delithiation shown in Fig. 2(b), we calculated the Grüneisen parameters and phonon lifetime of $Li_xNa_{1/4}FePO_4$ ($x = 3/4$, 1/2, 1/4, 0) at 300 K, which are illustrated in Fig. 4. As the Li-ion concentration x decreases, the value of the Grüneisen parameters decreases, which greatly decreases the intensity of phonon scattering, resulting in a significant increase in phonon lifetime and thermal conductivity.[44,45]

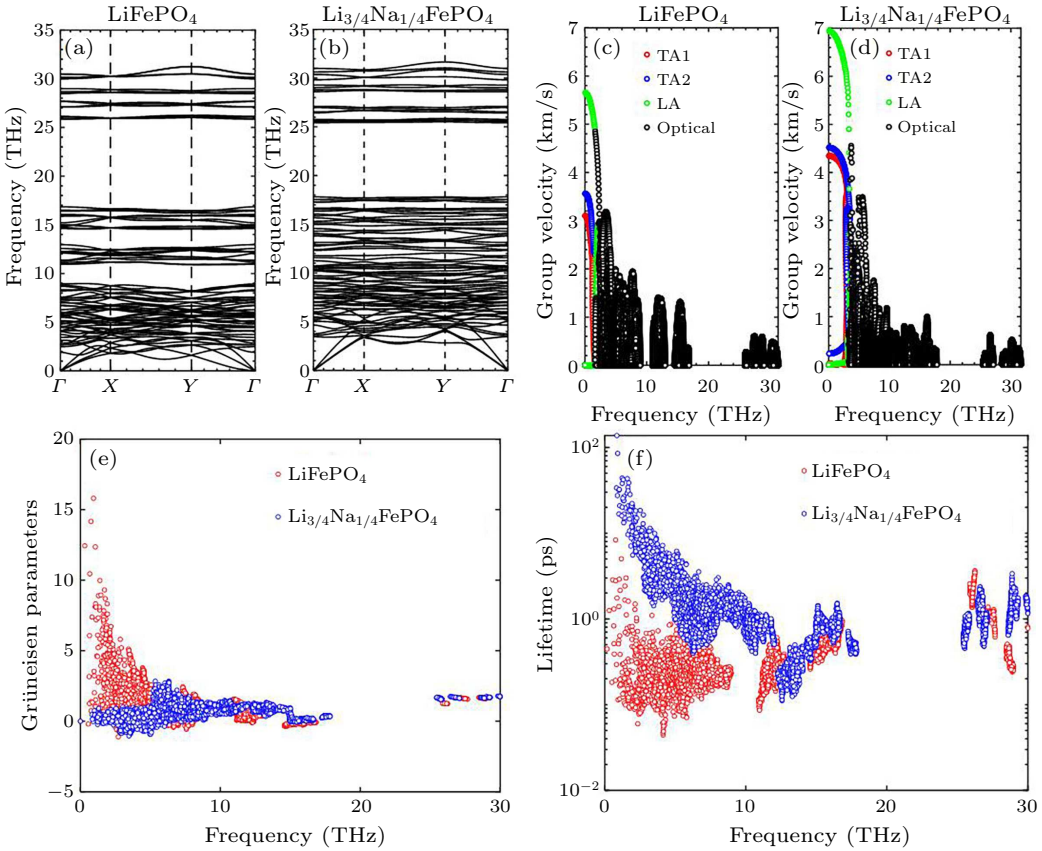


Fig. 3. (a), (b) Phonon dispersion curves, (c), (d) group velocity, (e) Grüneisen parameters and (f) phonon lifetime of $LiFePO_4$ and $Li_{3/4}Na_{1/4}FePO_4$ at 300 K.

To further compare the anharmonicity of $LiFePO_4$ and $Li_{3/4}Na_{1/4}FePO_4$, we analyzed the atomic bonding in terms. Each phosphate tetrahedron and each FeO_6 octahedron share a common edge in the $LiFePO_4$ structure. Due to the strong covalent nature of P–O bonds, all P–O and O–O distances are usually fixed. Since the Na atom has a larger diameter than the Li atom, Na substitution changes the Fe–O bond length of the FeO_6 octahedron, which affects the thermal conductivity.[46] Table 1 lists the bond lengths of all Fe–O bonds as well as the calculated average bond length and standard deviation (S) of all Fe–O bonds. The difference in thermal conductivity is related to the bonding interaction in the structure, which can be measured by the bond length. The bond strength and bond length have a negative correlation, and a strong bond is conducive to obtaining high thermal conductivity.[47] Furthermore, reducing the bond strength difference of the system is beneficial for eliminating the asymmetry of atomic vibration and improving the thermal conductivity.[48] The Fe–O bond length of $Li_{3/4}Na_{1/4}FePO_4$ is shorter than that of $LiFePO_4$, and the bond strength difference of the system is smaller than that of $LiFePO_4$, so $Li_{3/4}Na_{1/4}FePO_4$ has a higher thermal conductivity. From Table 1, the average bond length and standard deviation of $Li_{3/4}Na_{1/4}FePO_4$ are lower than those of $LiFePO_4$. This proves that the bonding strength of $LiFePO_4$ is mismatched in the system, while the bonding strength of $Li_{3/4}Na_{1/4}FePO_4$ is more matched in the system. In conclusion, the remarkable increase in thermal conductivity of $Li_{3/4}Na_{1/4}FePO_4$ is due to the low anharmonic effect caused by the small difference in bonding strength between atoms.

Table 1. Bond length of all Fe–O bonds, average bond length and standard deviation (S) of $LiFePO_4$ and $Li_{3/4}Na_{1/4}FePO_4$.

	Fe–O	
	$Li_{3/4}Na_{1/4}FePO_4$	$LiFePO_4$
Bond length (Å)	2.04	2.23
	2.05	2.13
	2.09	2.27
	2.03	2.06
	2.10	2.27
Average bond length (Å)	2.06	2.19
S (Å)	0.03	0.08

To verify this view, we quantified the bond strength of $Li_{3/4}Na_{1/4}FePO_4$ and $LiFePO_4$. We used DFT combined with the LOBSTER package[49] to calculate the crystal or-

bital Hamiltonian population (pCOHP) of the Fe–O bonds, as shown in Fig. 5(a). –pCOHP > 0 indicates that the electrons occupy the bonding orbitals, which is beneficial to bonding, while –pCOHP < 0 indicates that the electrons occupy the antibonding orbitals, which is not conducive to bonding.[50] As can be seen from Fig. 5(a), both $LiFePO_4$ and $Li_{3/4}Na_{1/4}FePO_4$ have bonding components, but the antibonding synthesis fraction of $LiFePO_4$ is much higher than that of $Li_{3/4}Na_{1/4}FePO_4$. This result proves our point that $Li_{3/4}Na_{1/4}FePO_4$ binds more strongly than $LiFePO_4$. In addition, the integral of pCOHP (denoted as ICOHP) can be used to quantitatively compare the strength of the bond, as shown in Fig. 5(b).[51] The results show that Na substitution can improve the bonding strength.

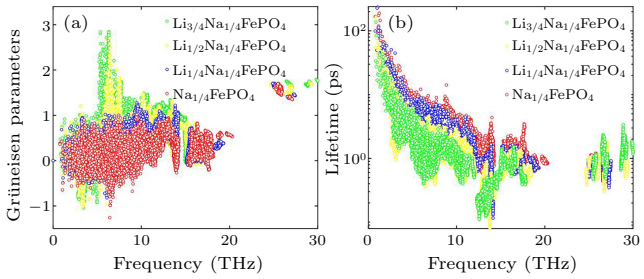


Fig. 4. (a) Grüneisen parameters and (b) phonon lifetime of $Li_xNa_{1/4}FePO_4$ ($x = 3/4$, 1/2, 1/4, 0) at 300 K.

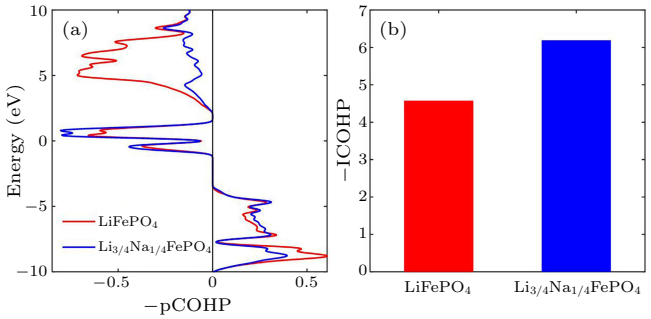


Fig. 5. (a) The –pCOHP and (b) –ICOHP of the Fe–O bonds.

4. Conclusion

In summary, we used the machine learning potential approach to systematically study the effects of Na substitution for Li on the thermal conductivity of $LiFePO_4$. We found that Na substitution can significantly improve the thermal conductivity, because the group velocity and the lifetime of $Li_{3/4}Na_{1/4}FePO_4$ are higher than those of $LiFePO_4$. In addition, the Fe–O bond length and the standard deviation of $Li_{3/4}Na_{1/4}FePO_4$ are shorter than those of $LiFePO_4$, so the strength between bonds is larger, and the bond strength difference of the system is smaller, which is conducive to eliminating nonharmonics and improving thermal conductivity of $Li_{3/4}Na_{1/4}FePO_4$. Moreover, the calculations of the Grüneisen parameters and phonon lifetime reveal that as the Li-ion concentration decreases, the phonon scattering decreases, the phonon lifetime increases and the thermal conductivity increases. Our findings establish a basic understanding of the heat transfer of $LiFePO_4$ batteries, and provide valuable guidance for improving the thermal conductivity of cathode materials.

Acknowledgements

This work was supported by the National Natural Science Foundation of China (Grant No. 12074115) and the Science and Technology Innovation Program of Hunan Province (Grant No. 2023RC3176).

References

[1] Nitta N, Wu F, Lee J T and Yushin G 2015 *Mater. Today* **18** 252
[2] Zhu T, Sternlicht H, Ha Y, Fang C, Liu D, Savitzky B H and Liu G 2023 *Nat. Energy* **8** 129
[3] Opitz A, Badami P, Shen L, Vignarooban K and Kannan A M 2017 *Renew. Sust. Energ. Rev.* **68** 685
[4] He L, Gu Z, Zhang Y, Jing H and Li P 2023 *Energy Fuels* **37** 4835
[5] Yan K, Chen Q, Zhang Z, Nie H, Wang R and Xu Z 2023 *Green Chemistry* **25** 9156
[6] Syed M A, Salehabadi M and Obrovac M N 2024 *Chem. Mater.* **36** 803
[7] Qiu X, Wang C, Xie L, Zhu L, Cao X and Ji X 2024 *J. Power. Sources* **60** 234365
[8] Yang C C, Jang J H and Jiang J R 2014 *Energy Procedia* **61** 1402
[9] Liu Y, Qin W, Zhang D, Feng L and Wu L 2021 *Progress in Natural Science: Materials International* **31** 14
[10] Xu J and Chen G 2010 *Physica B* **405** 803
[11] Wang Z H, Yuan L X, Wu M, Sun D and Huang Y H 2011 *Electrochim. Acta* **56** 8477
[12] Madram A R and Faraji M 2017 *New J. Chem.* **41** 12190
[13] Cong J, Luo S H, Li K, Wang J C, Wang Y F, Yan S X and Li P W 2023 *Ionics* **29** 3915
[14] Shah K, Vishwakarma V and Jain A 2016 *J. Electrochem. En. Conv. Stor.* **13** 030801
[15] Feng T, O'hara A and Pantelides S T 2020 *Nano Energy* **75** 104916
[16] Zhang Z and Cao B 2022 *Sci. China Phys. Mech. Astron.* **65** 117003
[17] Qian X, Gu X, Dresselhaus M S and Yang R 2016 *J. Phys. Chem. Lett.* **7** 4744
[18] Zhang Z, Guo Y, Bescond M, Chen J, Nomura M and Volz S 2022 *Phys. Rev. Lett.* **128** 015901
[19] Meng H, Yu X, Feng H, Xue Z and Yang N 2019 *Inter. J. Heat & Mass Trans.* **137** 1241
[20] Mistry A N, Palle H R and Mukherjee P P 2019 *Appl. Phys. Lett.* **114** 023901
[21] Wu C W, Ren X, Li S Y, Zeng Y J, Zhou W X and Xie G F 2022 *Appl. Phys. Lett.* **121** 172201
[22] Wu C, Huang W, Liu L, Wang H, Zeng Y, Xie J, Jin C and Zhang Z 2016 *CrystEngComm* **18** 7707
[23] Whittingham M S 2004 *Chem. Rev.* **104** 4271
[24] Padhi A K, Nanjundaswamy K S and Goodenough J B 1997 *J. Electrochem. Soc.* **144** 1188
[25] Kresse G and Furthmüller J 1996 *Phys. Rev. B* **54** 11169
[26] Kresse G and Furthmüller J 1996 *Computational Materials Science* **6** 15
[27] Kresse G and Joubert D 1999 *Phys. Rev. B* **59** 1758
[28] Perdew J P, Burke K and Ernzerhof M 1996 *Phys. Rev. Lett.* **77** 3865
[29] Ouyang Y L, Yu C, Yan G and Chen J 2021 *Front. Phys.* **16** 43200
[30] Liu Y, Liang H, Yang L, Yang G, Yang H, Song S, Mei Z, Csányi G and Cao B 2023 *Adv. Mater.* **35** 2210873
[31] Ouyang Y, Yu C, He J, Jiang P, Ren W and Chen J 2022 *Phys. Rev. B* **105** 115202
[32] Togo A and Tanaka I 2015 *Scrip. Mater.* **108** 1
[33] Li W, Carrete J, Katcho N A and Mingo N 2014 *Comput. Phys. Commun.* **185** 1747
[34] Shu Z, Xu H, Yan H and Cai Y 2024 *Front. Phys.* **19** 33202

[35] Zhu X L, Liu P F, Zhang J, Zhang P, Zhou W X, Xie G F and Wang B T 2019 *Nanoscale* **11** 19923
[36] Chen X K, Zhang E M, Wu D and Chen K Q 2023 *Phys. Rev. Appl.* **19** 044052
[37] Xie Z X, Chen X K, Yu X, Deng Y X, Zhang Y, Zhou W X and Jia P Z 2024 *J. Appl. Phys.* **135** 024302
[38] Zhou W, Cheng Y, Chen K, Xie G F, Wang T and Zhang G 2020 *Adv. Funct. Mater.* **30** 1903829
[39] Chen X K, Hu X Y, Jia P, Xie Z X and Liu J 2021 *Inter. J. Mech. Sci.* **206** 106576
[40] Zhu X L, Yang H, Zhou W X, Wang B, Xu N and Xie G F 2020 *ACS Appl. Mater. Interfaces* **12** 36102
[41] Gan Y, Wu C W, Xie Z X, Deng Y X, Zhang Y, Zhou W X and Chen X K 2022 *Langmuir* **38** 7733
[42] Zhu X L, Liu P Fm Xie G F and Wang B T 2019 *Phys. Chem. Chem. Phys.* **21** 10931
[43] Zhu X L, Liu P F, Xie G F, Zhou W X, Wang B T and Zhang G 2019 *Nanomaterials* **9** 597
[44] Jia P Z, Xie Z X, Deng Y X, Zhang Y, Tang L M, Zhou W X and Chen K Q 2022 *Appl. Phys. Lett.* **121** 043901
[45] Wu C W, Ren X, Xie G F, Zhou W X, Zhang G and Chen K Q 2022 *Phys. Rev. Appl.* **18** 014053
[46] Delmas C, Maccario M, Croguennec L, Le C F and Weill F 2008 *Nat. Mater.* **7** 665
[47] Lee S, Esfarjani K, Luo T, Zhou J, Tian Z and Chen G 2014 *Nat. Commun.* **5** 3525
[48] Zeier W G, Zevalkink A, Gibbs Z M, Hautier G, Kanatzidis M G and Snyder G J 2016 *Angew. Chem. Int. Ed.* **55** 6826
[49] Maintz S, Deringer V L, Tchougréeff A L and Dronskowski R 2016 *J. Comput. Chem.* **37** 1030
[50] Deringer V L, Tchougréeff A L and Dronskowski R 2011 *J. Phys. Chem. A* **115** 5461
[51] Liu X, Jiao Y, Zheng Y, Jaroniec M and Qiao S Z 2019 *J. Am. Chem. Soc.* **141** 9664